A Dual Mechanism for Low-Stress Hemolysis in Laminar Blood Flow

Human blood is sheared in cone-and-plate and parallel-plate rotational viscometers, the latter with variable plate spacings h. Plasma is analyzed for hemoglobin and LDH content before and after shearing to determine the extent of shear-induced blood damage within the low-stress regime (stress $\leq$ 13 Pa). Geometrical variations in the test apparatus can be accommodated by correlating blood damage with the radially-averaged shear rate. Data on expired blood are shown to imply that much of the damage arises in the bulk fluid, with a smaller contribution from surface effects. Models are proposed to explain these results, obtained over a shear rate range to 5,000 s^{-1}; parallel-plate platen separation is $0.25 < h < 1.00$ mm, cone-and-plate angle is 0.5°, and both systems have platens 100 mm in diameter.

R. L. BEISSINGER and M. C. WILLIAMS

Chemical Engineering Department
University of California, Berkeley
Berkeley, CA 94720

SCOPE

With the advent of prosthetic devices and artificial organs as major components of medical treatment has come widespread recognition that biocompatibility is a complex and limiting problem. The bioengineer designing these devices, and the medical practitioner using them, must be aware that the materials of construction and device dynamics both have the potential for adverse influence upon body tissues. Damage to blood is particularly important, and complicated by the fact that the tissue, in this case, is flowing. A multitude of chemical and mechanical interactions can occur between the device surface and the blood's plasma solutes and cellular components. Such interactions are influenced by hydrodynamic and geometric parameters of the device; these parameters may also act upon the blood independently of direct contact with device walls and materials. Separating the mechanisms from each other has proved to be difficult.

The most frequently reported measure of blood damage is hemolysis, the loss of hemoglobin from erythrocytes into the plasma. Hemolysis implies major cell damage because the hemoglobin molecule is too large to escape the erythrocyte without substantial deformation or rupture of the cell membrane. In clinical circumstances, device materials should be chosen and device hydrodynamics designed so that hemolysis is minimized. To this end, correlations of hemolysis with material chemical parameters (e.g., Monroe et al., 1980; Offeman and Williams, 1979a) are of practical utility. Engineering design requires also an understanding of such factors as fluid shear stress (Leverett et al., 1972) and shear rate (Shapiro and Williams, 1968), surface roughness and device edges and corners (Monroe et al., 1981), and other boundary and interface phenomena (e.g., Offeman and Williams, 1979b).

It is currently common to idealize flow-induced hemolysis by dividing this complex phenomenon conceptually into two regimes. A *high-stress regime* prevails when cell rupture occurs in the bulk fluid due to exposure to stress sufficiently high, sustained for a sufficiently long time (Leverett et al.); this is presumed to be independent of wall materials and device surface/volume ratio, to be nearly instantaneous, and not to be seen—in fresh normal bloods—at shear stresses less than about 150 Pa, this being the rupture threshold for long exposure times to stress. These stress conditions and associated massive cell damage are far more severe than found in desirable clinical conditions, for which damage is idealized as being in the *low-stress regime:* sensitive to wall material chemistry, proportional to device surface/volume ratio, having slow kinetics, and being controlled by fluid shear rate while essentially independent of shear stress.

Despite the conceptual utility of this two-regime idealization, there has been difficulty in basing engineering design upon these ideas. For example, it has never been demonstrated that hemolysis in one device can be predicted quantitatively from that in another, even in cases where the only differences apparently were geometrical scale factors. The low-stress idealization was tested by Offeman and Williams (1979b) with time-dependent data from rotating-disk devices; it was found not to be consistent with size scale variations of order 2 and disk speed variations of order 3. However, those devices were complicated by the presence of a substantial reservoir of blood beyond the disk edge, which may have contributed a nontrivial amount of hemolysis.

In the present study we investigate the low-stress regime under more carefully controlled conditions. Two rotating-surface geometries are employed, the parallel-plate and cone-and-plate systems common in viscometric work, and the former is used to secure further geometrical variation by change of the plate spacing. Viscosity data are obtained in the same devices. Erythrocyte damage is represented in terms of plasma concentrations of both hemoglobin and a specific cell enzyme, LDH, in an effort to determine whether damage parameters can be shared for different components of the cell. All device surfaces are of the same material (stainless steel) and test volumes are not depleted by sampling during runs.

CONCLUSIONS AND SIGNIFICANCE

Erythrocyte loss of hemoglobin and the enzyme could be correlated in terms of the radial-averaged shear rate, the same curve of damage vs. average shear rate resulting from data taken with cone-and-plate and parallel-plate systems having similar diameters and gap spacings at the rim. Such a result could emerge from either a surface-controlled mechanism or a bulk-flow mechanism, in these geometries, since shear rate variations (when they exist) are principally in the radial direction and not in the direction normal to the bounding surfaces. Variation of spacing between the parallel plates showed that a weak sensitivity to surface/volume ratio existed, but that the major source

Correspondence concerning this paper may be addressed to either M. C. Williams or R. L. Beissinger. R. L. Beissinger is presently Assistant Professor of Chemical Engineering at Illinois Institute of Technology, Chicago

of damage for these older bloods was in the bulk fluid rather than at the solid surface.

Such a result is incompatible with the low-stress idealization described above, requiring instead the hypothesis that surface and bulk mechanisms for damage act simultaneously with a relative importance that depends on blood chemistry (including changes during storage) and surface material chemistry. This concept has not been proposed before, but is consistent also with certain other reports available. One possible interpretation is that fresh blood, being resistant to the bulk-flow mechanism, will sustain damage primarily due to device surface interaction; older blood, still usable for transfusions, will suffer damage in greater proportion from bulk flow phenomena. A "parallel" model for the overall hemolysis kinetic process is provided for purposes of illustration and semiquantitative discussion, and a new "series" model is proposed.

INTRODUCTION

The flow of blood in artificial organs, implanted or extracorporeal, is usually accompanied by various forms of blood damage. One important measure of damage is hemolysis, the release of intracellular hemoglobin from erythrocytes into the surrounding plasma. Not only does this imply that major alterations of many kinds have occurred in the red cell, but in a clinical sense it represents a condition of induced anemia in the patient. Moreover, the free hemoglobin is identified by the body as a foreign substance, thus placing an additional burden on the body organs of an already-ill individual; under extreme conditions a toxic concentration level can be reached. It is important, therefore, that the engineer designing artificial organs understand the chemical and mechanical factors affecting hemolysis and related forms of damage to blood in flow.

It was demonstrated very early (Nevaril et al., 1968) that if shear stress in the flowing blood is sufficiently high, massive hemolysis can result. Such *high-stress* hemolysis, accompanied by gross morphological changes and rupture of the cells, is idealized as being nonexistent at stresses below about 150 Pa (for fresh normal human blood). Above this threshold, hemolysis is a steeply increasing function of stress, occurs very rapidly, and is independent of the chemical or physical nature of device walls. Much higher stresses than this can be withstood for very short times, presumably because of cell viscoelastic properties, as shown by the stress/time map of Leverett et al. (1972). These mechanical features of hemolysis were reviewed by Hellums and Brown (1977) and earlier by Blackshear (1972).

In normal clinical circumstances, these high stresses are usually avoided. However, even in the *low-stress* regime hemolysis can be a problem, and this is the domain of the present investigation. Experimental evidence indicates that such hemolysis correlates with shear rate rather than with shear stress, even for older stored bloods (Shapiro and Williams, 1970). It is believed to occur at or near the solid synthetic surface (Blackshear, 1972), the strongest evidence being its sensitivity to surface chemistry (Nyilas et al., 1970; Bernstein, 1971; Lampert and Williams, 1972; Offeman and Williams, 1979a; Monroe et al., 1980) and to surface morphology, especially roughness (Offeman and Williams, 1979a; Wielogorski et al., 1976; Monroe et al., 1981).

The kinetics of low-stress hemolysis are rather slow, being highest at the onset of shear and slowing thereafter; numerous plots of plasma hemoglobin concentration vs. time, when various biomaterial surfaces were used for shearing, have been presented by this laboratory. These kinetic hemolysis curve (KHC) kinetics have been correlated, for polymeric surfaces, with the critical surface energy of those plastics (Lampert and Williams, 1972; Offeman and Williams, 1979a). This material effect is evident despite the fact that plasma proteins adsorb onto synthetic surfaces, thereby rendering them less damaging (Bernstein et al., 1966; Nichols and Williams, 1976). Studies of protein adsorption kinetics (Beissinger and Leonard, 1982) show a time scale corresponding to the short-time rapid change of the KHC, which would seem to reinforce speculation (Blackshear, 1972) that the KHC is merely a reflection of the protein deposition. However, Offeman and Williams (1979b) demonstrated directly that this is not entirely so, and that the KHC curvature probably is a manifestation of the sequential hemolysis of cells having a distribution of fragilities within the sample tested.

While these hemolysis observations have been conveniently compartmentalized into regimes of high or low stress, the engineer must realize that device design cannot be entirely successful if based wholly on such idealizations. For example, Bacher and Williams (1970) took capillary flow data in the high-stress regime but observed materials-related trends associated with the capillary wall. It is also reasonable to expect that the important low-stress regime is characterized by damage mechanisms having their sources in both the bulk fluid and the device surface. For example, we have noted that wall materials effects in low-stress hemolysis seem to be proportionately more distinct with fresh blood samples than with old blood samples, suggesting the existence of a bulk flow mechanism that happens to be more influenced by storage trauma (Offeman and Williams, 1976) than is the surface mechanism. Furthermore, low-stress experiments with rotating disks having a blood reservoir beyond the disk edge show that beveling the edge (thus influencing local bulk hydrodynamics) increases hemolysis markedly, although surface area is not changed in the same proportion (Monroe et al., 1981). The reservoir itself appears to be the source of significant damage, as noted first by Nichols (1975). This was discussed by Monroe et al. (1981) in terms of the bulk stress discontinuities at the disk edge, experienced by cells circulating between the intradisk gap and reservoir.

A test of understanding blood damage in flow is to determine whether data obtained in one flow device can be used to predict data in another. Thus far, such capability has not been demonstrated. Offeman and Williams (1979b), using two rotating disk systems scaled for geometric and dynamic similarity, were unsuccessful in using a purely surface damage mechanism to interpret hemolysis. The KHC's for the two sizes, and for different rotational speeds, were not related as expected from surface models alone. Again, however, the existence of the blood reservoir complicated results and the lack of success could have stemmed from this.

In the present study, then, we determine to avoid reservoir complications by working with rotating geometries that contain the blood entirely within the controlled shearing surfaces. Two viscometric flows are established, a cone and plate and a parallel plate (resembling the rotating disk used in this laboratory in previous work), and the latter is varied by changing the plate spacing. The objective is to relate quantitatively the blood damage in one geometry to that in the other, and also to assess the degree to which surface effects and bulk effects contribute simultaneously. Finally, a step is taken towards extending hemolysis results to other chemical features of blood damage, by tracking also the release of cellular lactate dehydrogenase (LDH).

EXPERIMENTAL

Apparatus

A Weissenberg Rheogoniometer Model 17 (Sangamo; Sussex, England) was used both for viscometric characterization of the blood and for provision of shearing in blood damage studies. Blood was contained between two

TABLE 1. HYDRODYNAMIC PARAMETERS IN STEADY VISCOMETRIC FLOW*

Device	Shear Stress	Shear Rate
Cone and Plate	$\tau_{\phi\theta} = 3T/2\pi R^3 = \eta\dot{\gamma}_{\phi\theta}$	$\dot{\gamma}_{\phi\theta} = \Omega/\psi$
Parallel Plates	$\tau_{z\theta}(r) = \eta(r)\cdot\dot{\gamma}_{z\theta}(r)$	$\dot{\gamma}_{z\theta} = \Omega r/h$
(Rotating Disk)	$\tau_R = \frac{3T}{2\pi R^3}\left[1 + \frac{1}{3}\frac{d\ln T}{d\ln\Omega}\right]$ $= \eta(\dot{\gamma}_R)\cdot\dot{\gamma}_R$	$\dot{\gamma}_R = \Omega R/h$

* Valid for both Newtonian and non-Newtonian fluids, with raw data of the form $T(\Omega)$. Being in the viscometric limit, $\dot{\gamma}_{ij}$ components here correspond to notation $\dot{\gamma}^{\circ}$ used in the text.

horizontal platens, the lower being rotated at controlled angular speed Ω and the upper being stationary while registering a torque signal by the twist of a torsion bar sensed by a displacement transducer. For the cone-and-plate system (CP), the platens were 100 mm in diameter with the lower one having a cone of angle 0.52°. Parallel-plate systems (PP) were also 100 mm in diameter, with gaps being set at h = 0.25, 0.50, or 1.00 mm.

In these geometries, the steady-flow laminar hydrodynamics for Newtonian fluids are known exactly (ignoring edge effects at the free surface) and for non-Newtonian fluids approximately. Expressions for shear stress τ and shear rate $\dot{\gamma}$ are given in Table 1, in the classical viscometric limit of negligible inertia and absence of secondary flows. In this approximation, τ and $\dot{\gamma}$ in the CP system are independent of position; in the PP system $\dot{\gamma}$ is linear in r but independent of z, while $\tau(r)$ depends on fluid viscosity and is linear with r in the Newtonian limit. We will subsequently discuss the extent to which these approximations were valid in this work.

The rheogoniometer was also used to obtain the viscoelastic property of complex viscosity, $\eta^* = \eta' - i\eta''$, as a function of frequency ω of the oscillating lower platen. Here, η' is related to energy dissipation and η'' to energy storage during this sinusoidally varying shear flow. Measurements of the amplitude ratio and phase lag between the two platens were converted by standard methods (Walters, 1975) to η' and η'', for both the CP and PP systems.

All shearing surfaces were stainless steel, exposed to blood during repeated testing so that a monolayer of plasma protein was present at the beginning of each test. These surfaces were cleaned between runs with a phosphate detergent (Sparkleen; Fisher Scientific), rinsed and soaked in distilled water, and air-dried at ambient conditions; the protein monolayer remained intact during this experience.

Blood

Three blood samples were obtained in legally expired condition from the Alameda-Contra Costa Blood Bank, Oakland. Each had been stored there in a sterile blood bag for 21 days, with citrate-phosphate-dextrose preservative, at 4°C; it was normally tested in our laboratory within the next 1–5 days. In one case, a fresh venous sample was obtained from a fasted adult donor and stored under identical conditions in this laboratory for a similar duration. No qualitative differences were noted between these four bloods, in rheology or hemolysis. For this reason and because our major results stem from changing the flow geometry and hydrodynamics, we select here only one representative blood (sample BB3) to be discussed in detail below.

Procedure

The blood bag was gently inverted to assure homogenization of cells throughout the blood, then the test sample (1–5 mL) was transferred by slow gravity feed through blood bag tubing onto the lower platen and distributed across it by bringing down the upper platen to its predetermined operating position. Shearing was conducted for a specified time and at a specified rate, each such run representing a single datum in one of two types of test sequences: either a fixed-time shearing (10 min) at a series of $\dot{\gamma}$, or a fixed-rate shearing for various durations up to 30 min. The latter tests, establishing the KHC, are not germane to the present discussion and will be reported elsewhere (Beissinger and Williams). From the former tests, under certain conditions, viscosities could be obtained as $\eta = \tau/\dot{\gamma}$ during each run. Stress levels never exceeded 23 Pa in data reported here.

Experiments were conducted in a closed room at ambient conditions. Samples equilibrated thermally to ~21°C rapidly, before each run, due to the high platen heat capacity and small platen separation. In each geometry, a free blood/air interface existed at the rim. Whereas such an interface is known (Hellums and Brown, 1977) to cause certain blood alterations—e.g., plasma protein denaturation—it was deemed of little consequence here. Its extent was always small, only ~2% of all blood surface for the PP system at h_{max} = 1.00 mm and ~1% for the CP system. Furthermore, control tests described below indicated that static exposure to the air interface caused negligible damage.

Chemical analysis was performed for each run on samples taken from the blood bag directly, from a nonsheared control volume that was loaded into the apparatus and resided there for a time equal to a normal run duration, and from the regular sheared volume after the run. A wide spectrum of tests on the plasma was obtained from the Alta Bates Hospital Laboratory, requiring that essentially the entire volume of the sheared sample be used. From that spectrum, the most notable correlation with shearing was with LDH and therefore only those data are reported here. A short discussion of other chemical changes during similar tests has been given by Monroe et al. (1980).

Analysis for plasma hemoglobin was performed in our laboratory using a modified Crosby-Furth colorimetric method with reagent tetramethyl benzidine (noncarcinogenic) as described by Standefer and Vanderjagt (1977). Hematocrits were also obtained, by the standard centrifugation of samples in microcapillaries and subsequent reading of sedimented red cell volume fractions.

RESULTS AND DISCUSSION

Viscosity and Stress

Collectively, the viscometric data for both $\eta(\dot{\gamma})$ and $\eta^*(\omega)$ showed agreement among all geometries used, thus demonstrating that true material properties were being measured and geometry artifacts were not involved. Negligible change in η (i.e., in torque measurement) was noted during the 10-minute shearing period for any blood, despite significant hemolysis occurring. This is consistent with a picture wherein the formed elements in the blood were not changing geometrically during the course of erythrocyte damage. Indeed, optical microscopic examination of sheared blood was unable to detect any cell fragmentation or even morphological changes of the sort associated with high-stress hemolysis (Nevaril et al., 1969). The constancy of η also implies that cell sedimentation was avoided or, at least, did not create significant inhomogeneities in the blood during these relatively short tests.

Rheological measurements are presented and discussed in more detail elsewhere (Beissinger and Williams). Data on η and $|\eta^*| = |(\eta')^2 + (\eta'')^2|^{1/2}$, for sample BB3, taken in the the PP geometry, are displayed in Figure 1. The intradisk gap here is small enough (h = 0.25 mm) so that secondary hydrodynamics in steady flow are negligible, as will be demonstrated in the Appendix, and the viscometric approximation $\dot{\gamma}(r) = \Omega r/h$ is legitimate for even the highest $\dot{\gamma}$ achieved. Because of the consequent non-Newtonian $\eta(r)$ variation, the basic function $\eta(\dot{\gamma})$ had to be extracted from data on torque T vs. $\dot{\gamma}_R = \Omega R/h$ by the standard method (Walters, 1977):

$$\eta(\dot{\gamma}_R) = \frac{T}{2\pi R^3\dot{\gamma}_R}\left[3 + \frac{d\ln(T/2\pi R^3)}{d\ln\dot{\gamma}_R}\right]. \qquad (1)$$

Values of η in Figure 1 are in the commonly reported range (Dintenfass, 1971), and the degree of non-Newtonian character is small enough that subsequent appeals to Newtonian fluid mechanics (Appendix) will be relevant if not exact.

Figure 1 shows that viscometry stress levels, identical to the highest-τ blood damage runs, were always low. The highest-$\dot{\gamma}$ point in Figure 1 corresponds to τ = 22 Pa, and blood damage was only assessed to $\dot{\gamma}_R \cong 3{,}700\ s^{-1}$ in PP and $\dot{\gamma} = 4{,}120\ s^{-1}$ in CP (corresponding to $\tau \cong 13$ Pa, from Figure 1). This very low stress level, together with the stable viscosity level during 10 minutes of shearing, indicates that the low-stress regime (i.e., hemolysis without cell rupture) was indeed attained even for this aged sample of blood.

The display of $|\eta^*|$ in Figure 1 is included for diagnostic purposes. As for many other fluids, $|\eta^*(\omega)|$ for blood is seen—by extrapolation, in this case—to be functionally very similar to $\eta(\dot{\gamma})$, with $|\eta^*| \leq \eta$ for all $\omega = \dot{\gamma}$ in which true flow occurs. This relationship (Cox and Merz, 1958) is useful for characterization if low-$\dot{\gamma}$ measurements cannot be made, as was the case here. The upswing

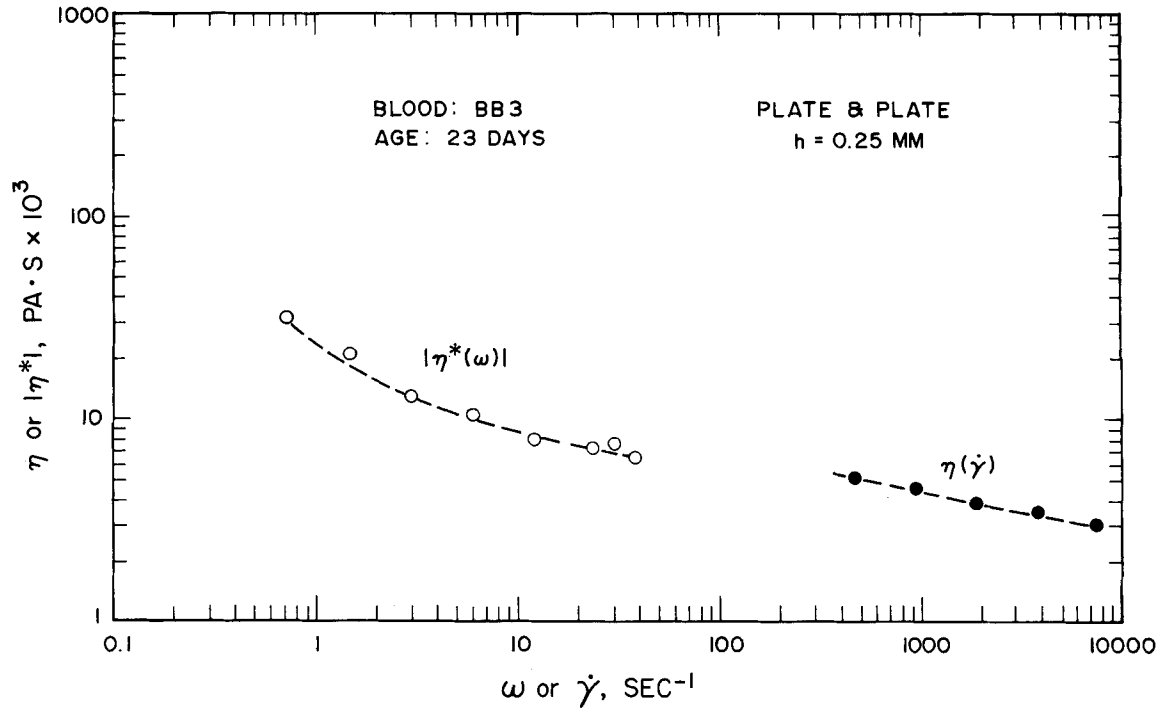

Figure 1. Non-Newtonian viscosity $\eta(\dot{\gamma})$ and magnitude of the complex viscosity $\eta^*(\omega)$. Both obtained in the parallel plate device with $h = 0.25$ mm. In the blood damage tests, $\dot{\gamma}$ was sufficiently high throughout most of each device that the blood was nearly Newtonian according to the data above.

in $|\eta^*|$ at low ω reveals the presence of a yield stress, a potentially useful feature for correlation purposes even though its influence on the bulk hydrodynamics at higher $\dot{\gamma}$ may be negligible.

Blood Damage

Control tests run on each blood established that the blood loading into the shearing device, plus the unloading associated with sample collection, plus nonflow aging for the standard 10 min, all led to a baseline level of plasma hemoglobin c_o; this was usually the same or only slightly larger than the initial level in the blood bag. Values of c_o were used as the $\dot{\gamma} = 0$ intercept of plots of c vs. $\dot{\gamma}$.

The presentation of damage information obtained in two different geometries, as a function of flow intensity parameters, requires in itself some concept of the damage mechanism. We begin by adopting the currently-accepted belief that low-stress blood damage occurs at device walls and is controlled by the magnitude of $\dot{\gamma}$ at the wall. If the total hemoglobin release is a surface-dominated phenomenon, it should be represented in terms of an integral over all solid surfaces. Thus, a reasonable correlation parameter might be the surface-averaged shear rate $\langle\dot{\gamma}\rangle_S$. For the parallel-plate device (PP), this is

$$\langle\dot{\gamma}\rangle_S \equiv \frac{1}{2\pi R^2}\left[2\pi\int_0^R \dot{\gamma}(r)|_o r\,dr + 2\pi\int_0^R \dot{\gamma}(r)|_h r\,dr\right] \ldots .PP \quad (2)$$

where the two integrals represent conditions at the two surfaces $z = 0$ and $z = h$. A similar expression prevails for the CP, although here $\dot{\gamma}(r)$ is not as strongly r-dependent as for the PP (and, in the viscometric limit, $\dot{\gamma}$ is independent of r). In general, the integrand $\dot{\gamma}(r)$ should be interpreted as the absolute magnitude of the strain rate tensor $\dot{\gamma}$, thus $|\dot{\gamma}| = (\frac{1}{2}\Sigma_{i,j}\dot{\gamma}_{ij}^2)^{1/2}$; this accommodates all existing strain rate components $\dot{\gamma}_{ij}$, including those arising when secondary flows and related tensile components are important. This is merely definitional in calculating $\langle\dot{\gamma}\rangle_S$, reflective of the total intensity of strain experienced by cells, and makes no statement about cell response to various $\dot{\gamma}_{ij}$ components explicitly.

In the limit of viscometric (creeping) flow described in Table 1, the CP geometry gives $\dot{\gamma} = \dot{\gamma}^o_{\phi\theta} = \Omega/\psi$ so that the averaging process is trivial and $\langle\dot{\gamma}^o\rangle_S = \Omega/\psi$. This is not so in the PP viscometric case, where $\dot{\gamma} = \dot{\gamma}^o_{z\theta} = \Omega r/h$ and thus $\langle\dot{\gamma}^o\rangle = 2\dot{\gamma}^o_R/3$. The degree to which the latter relationship approximates the PP operating conditions in these tests is demonstrated in Table 2, based upon the Newtonian-flow analysis in the Appendix. With $h = 0.25$ mm, secondary flows were always small and $\langle\dot{\gamma}\rangle_S = \langle\dot{\gamma}^o\rangle_S$ for all practical purposes; this was the condition under which the viscosity data of Figure 1 were obtained. For $h = 0.5$ mm, the approximation $\langle\dot{\gamma}\rangle_S \cong \langle\dot{\gamma}^o\rangle_S$ is still remarkably good, being within 4% of the exact evaluation of Eq. 2 even at $\Omega = 37.7$ rad/s despite a large $\dot{\gamma}_{zr}$ component and z-asymmetries in the $\dot{\gamma}_{ij}(r,z)$ pattern. For $h = 1.0$

TABLE 2. SURFACE-AVERAGE SHEAR RATES IN PARALLEL-PLATE ROTATIONAL FLOW*

h, mm	Ω rad/s	Shear Rates, s^{-1}					
			$\dot{\gamma}^o_{z\theta}\|_R$	$\dot{\gamma}_{z\theta}\|_R$	$\dot{\gamma}_{zr}\|_R$	$\langle\dot{\gamma}\rangle_S$	$\langle\dot{\gamma}^o\rangle_S$
0.25	9.42	0	1885	1885	−22	1257	1257
		0.25	1885	1885	−32		
	18.8	0	3770	3769	−90	2515	2513
		0.25	3770	3773	−135		
	37.7	0	7540	7537	−359	5040	5025
		0.25	7540	7554	−538		
0.50	9.42	0	942	942	−45	630	629
		0.50	942	945	−67		
	18.8	0	1885	1881	−180	1270	1257
		0.50	1885	1901	−270		
	37.7	0	3770	3734	−720	2616	2513
		0.50	3770	3906	−1077		
1.00	9.42	0	471	467	−90	327	315
		1.00	471	487	−135		
	18.8	0	942	903	−358	723	629
		1.00	942	1075	−527		
	37.7	0	1885	1560	−1434	1921	1257
		1.00	1885	2937	−2154		

* See Appendix for analytical details. In all cases $R = 5.0$ cm and $\nu = \eta_o/\rho = 0.035/1.05 = 0.033$ cm^3/s, in this Newtonian-flow analysis.

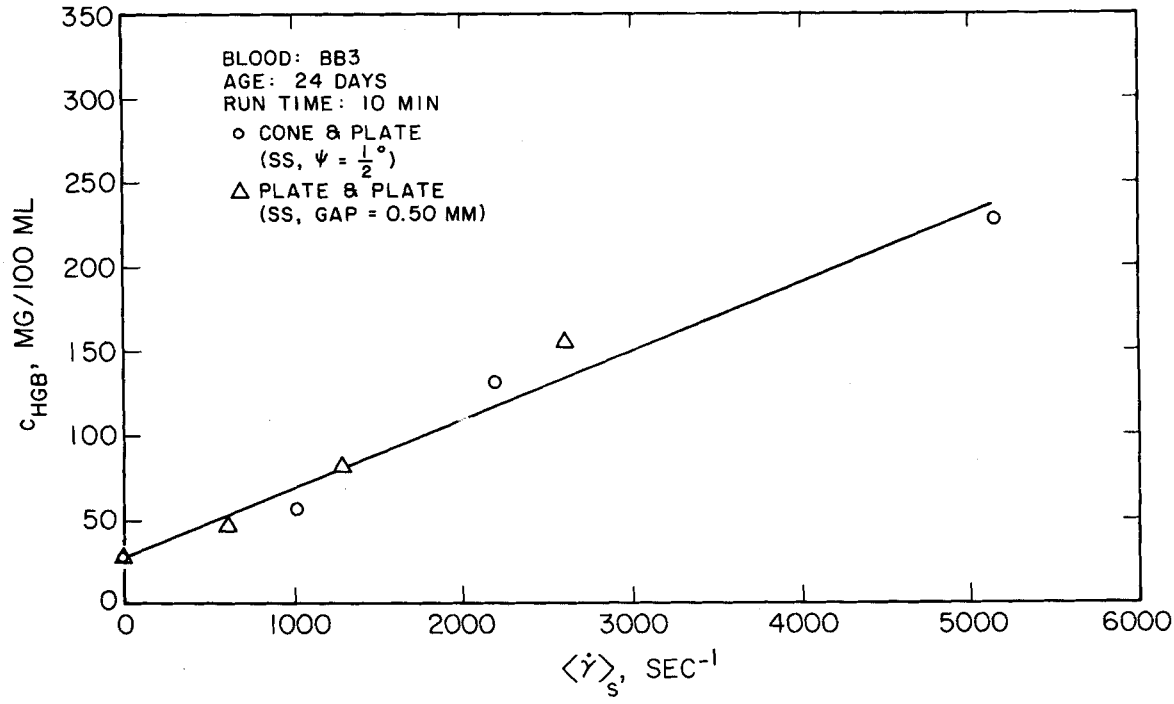

Figure 2. Change of plasma hemoglobin concentration with increasing platen speed Ω, the latter represented in terms of radially-averaged shear rate $\langle\dot{\gamma}\rangle_S$ (or $\langle\dot{\gamma}_B\rangle$) for both the parallel-plate and cone-and-plate devices.

mm, however, deviations are noted even for $\Omega = 9.4$ rad/s and the full form of $|\dot{\gamma}|$ is needed for evaluating $\langle\dot{\gamma}\rangle_S$; at $\Omega = 37.7$ rad/s $\langle\dot{\gamma}^o\rangle_S$ is exceeded by 53%.

One type of test of the proposed correlation of blood damage with $\langle\dot{\gamma}\rangle_S$ is seen in Figure 2, where the PP and CP hemolysis data are seen to coincide reasonably well. Similar success is enjoyed with LDH release data in Figure 3. In these cases, the intrinsic geometrical differences between the two systems are under scrutiny. Scale effects are eliminated by using the same platen diameters and comparable gaps at the rim ($h = 0.50$ mm for PP, $h_R = 0.45$ for CP). Under these conditions, it happens that viscometric flow is well approximated in both geometries for $\langle\dot{\gamma}\rangle_S \lesssim 1{,}500\ s^{-1}$. Above this, divergence from $\langle\dot{\gamma}^o\rangle_S$ increases for both but faster for CP than for PP. At the highest Ω (37.7 rad/s), $\langle\dot{\gamma}\rangle_S$ exceeds $\langle\dot{\gamma}^0\rangle_S$ by only 4% in the PP but by 24% in the CP. As shown in the Appendix, the CP flow develops several secondary $\dot{\gamma}_{ij}$, and the primary component $\dot{\gamma}_{\theta\phi}$ is grossly distorted with θ. The corresponding PP shear has only one large secondary component, $\dot{\gamma}_{zr}$, and the primary term $\dot{\gamma}_{z\theta}$ is only slightly affected. Given these differences, the correlation with such a simple parameter as $\langle\dot{\gamma}\rangle_S$ for the two geometries is gratifying.

However, superposition of data in Figures 2 and 3 does not signify that blood damage is surface-dominated here. Since $\dot{\gamma}_{ij}(r,z)$ components in the bulk pP flow have the same r-dependence as those at the surfaces and z-dependence remains small, a *volume*-averaged shear rate—presumably characterizing damage mechanisms in the bulk fluid—would show similar correlative success.

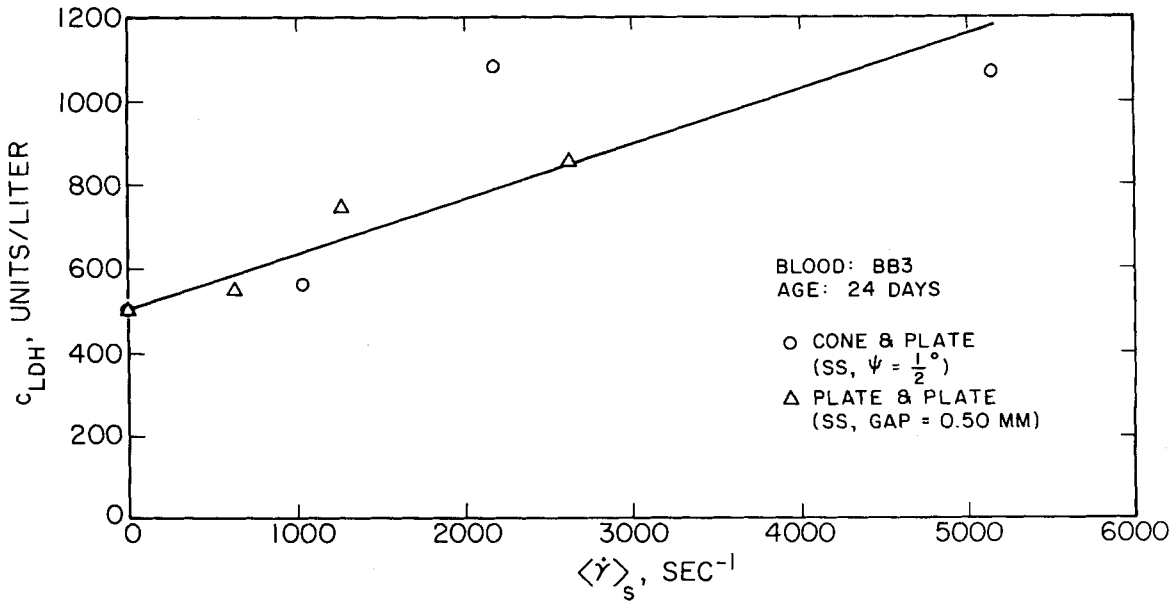

Figure 3. Change of plasma LDH concentration with increasing platen speed Ω, the latter represented in terms of the radially-averaged shear rate $\langle\dot{\gamma}\rangle_S$ (or $\langle\dot{\gamma}_B\rangle$) for both the CP and PP devices.

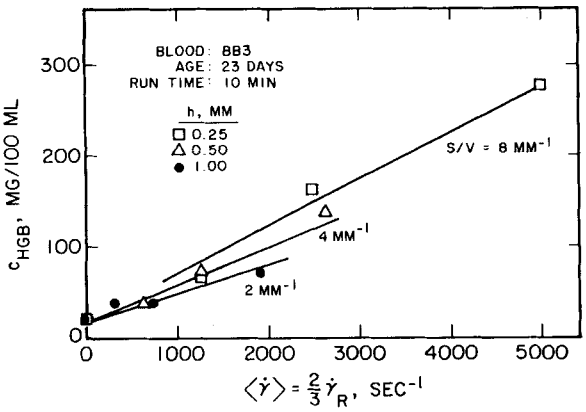

Figure 4. Change of plasma hemoglobin concentration with radially-averaged shear rate in the PP device, for three different interplaten spacings h (corresponding to different metal surface/blood volume ratios S/V). The three lines drawn here represent the best global fit of all the data, using Eq. 5 with $\lambda = 0.36$ and $\bar{K} = 2.05 \times 10^{-4}\text{mm}^{-\lambda}\text{-min}^{-1}$.

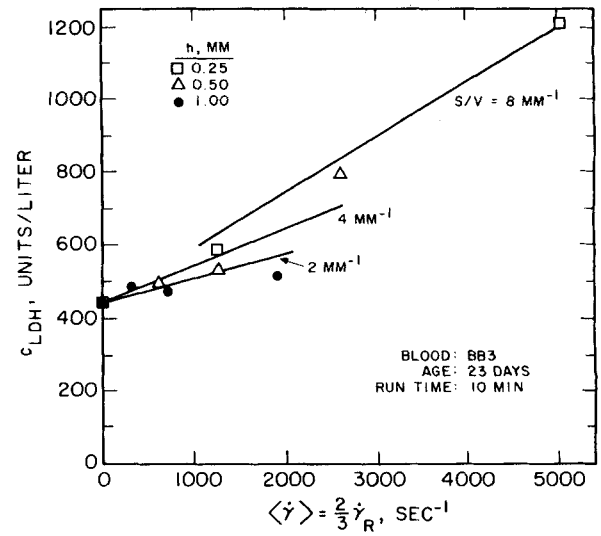

Figurer 5. Same as Figure 4, but for LDH concentration. Lines are drawn using $\lambda = 0.58$ and $\bar{K} = 5.18 \times 10^{-5}\text{mm}^{-\lambda}\text{-min}^{-1}$.

A second type of geometric change was obtained by varying h in the next set of PP experiments. Surprisingly, blood damage expressed as plasma concentration (c_{HGB} or c_{LDH}) was almost independent of h, despite h (and surface-to-volume ratio) changing by a factor of 4.0. This is entirely inconsistent with a surface-dominated phenomenon. To illustrate more precisely, suppose that surface-generated hemolysis is proceeding at the wall so that a *local* flux of free hemoglobin moving into the plasma is given by

$$j(r) = K_S\dot\gamma(r) \text{.....} z = 0, h \qquad (3a)$$

(Linear proportionality to $\dot\gamma$ in Eqs. 3–7 is primarily a convenience for illustration purposes. Figures 2–5 show that it is a fairly good approximation.)

Then, the total release rate is

$$w = \int j dS = 4\pi K_S \int_0^R \dot\gamma(r)|_S r dr = K_S\langle\dot\gamma\rangle_S S \qquad (3b)$$

where K_S includes surface-related kinetic factors and S is total solid surface area. The change of plasma hemoglobin concentration due to shear is then

$$\Delta c = \frac{\int_0^{t_0} w dt}{V(1-H)} = \left(\frac{S}{V}\right)\frac{\langle\dot\gamma\rangle_S}{(1-H)}\int_0^{t_0} K_S(t)dt \qquad (3c)$$

using H for hematocrit (cell volume fraction in the blood) and V for total blood volume, equal to $\pi R^2 h$ in the PP system. In this context, it is clear why our results showing Δc to be nearly independent of h (i.e., S/V) are incompatible with having a surface mechanism alone. Furthermore, the successful superpositions (Figures 2 and 3) of Δc vs. $\langle\dot\gamma\rangle$ from the two geometries were achieved despite S/V equalling 4.0 mm^{-1} in the PP system and 6.8 mm^{-1} in the CP system, a discrepancy which should have destroyed the correlation according to Eq. 3c.

An alternative model would be the bulk-flow one, akin to homogeneous chemical reactions with rates expressed on a unit volume basis:

$$\mathcal{R}(r) = K_B\dot\gamma(r) \text{.....all } z \qquad (4a)$$

with a kinetic coefficient K_B accommodating mechanisms in the bulk fluid. Then,

$$\Delta c = \frac{\int\int \mathcal{R} dV dt}{V(1-H)} = \frac{\langle\dot\gamma\rangle_B}{1-H}\int_0^{t_0} K_B(t)dt \qquad (4b)$$

and no S/V dependence appears. The two models (surface and bulk) of Eqs. 3c and 4b can be assessed quantitatively by using each to compute their respective time-average rate constants $\bar{K} = \int K(t)dt/t_o$, for the 10-minute runs with PP and CP tests. A regression procedure based on a finite difference Levenberg-Marquardt algorithm was used to give a best fit, separately, to the data of Figures 2 and 3, as well as to the variable-h data of Figures 4 and 5. The full form of $\dot\gamma(r) = |\dot\gamma(r)|$ was used for computing $\langle\dot\gamma\rangle$ in both Eqs. 3c and 4b; $\dot\gamma_{ij}(r)$ are displayed in Table 2 and the Appendix.

Results are given in Table 3. In the variable-h PP data, it is clear that the two "constants" $\bar{K}_S$ and $\bar{K}_B$ both vary with S/V, though in opposite directions. This indicates that neither a purely-surface nor a purely-bulk mechanism is correct. In the comparison of PP and CP data, the two $\bar{K}_S$ values are grossly different though the

TABLE 3. KINETIC PARAMETERS FOR BLOOD DAMAGE MODELS (USING $\Delta c \propto \langle\dot\gamma\rangle$)

Blood* Age	Geometry	h, mm	S/V, mm^{-1}	$\bar{K}_S \times 10^6$ mg_{HGB}/cm^2	$\bar{K}_B \times 10^5$ mg_{HGB}/cm^3
23 days	Parallel plate	0.25	8	0.67	5.39
	Parallel plate	0.50	4	1.15	4.60
	Parallel plate	1.00	2	1.38	2.75
24 days	Parallel plate	0.50	4	1.24	4.94
	Cone and plate	($\psi = 0.52°$) $h_R = 0.454$	6.87	0.61	4.21

* Sample BB3, sheared for 10 min.

two $\overline{K}_B$ values are similar. The latter observation encourages the conclusion that the bulk mechanism is dominant in these tests; moreover, the variable-h PP cases show that $\overline{K}_B$ values were comparable for $h = 0.25$ and 0.50 mm (minimal complications from secondary flows), while $\overline{K}_S$ values differed considerably even there.

A demonstration of the coupling of surface and bulk mechanisms in blood damage is provided by correlating the variable-h PP data with the two-parameter $(\lambda, \overline{K})$ function

$$\frac{\Delta c}{c_{\max}} = \left(\frac{S}{V}\right)^{\lambda} \frac{\langle\dot{\gamma}\rangle}{\langle\dot{\gamma}\rangle_{\max}} \frac{\overline{K} t_0}{(1-H)} \tag{5}$$

Here, the use of $\langle\dot{\gamma}\rangle_{\max}$ (always 5,040 s^{-1}) and $c_{\max}$ (measured, for $S/V = 8$ mm^{-1}) is merely a dimensional convenience, and $t_o = 10$ min. Variation of λ accommodates the cases of both Eq. 3c (when $\lambda = 1$) and Eq. 4b (when $\lambda = 0$). The resulting correlation is shown by solid lines in Figures 4 and 5. The global least-squares curve fit for hemolysis in Figure 4 is achieved with $\lambda = 0.36$ and $\overline{K} = 2.05 \times 10^{-4}$ $mm^{-\lambda}\cdot min^{-1}$, the sum of squared residuals being 0.013. Identical treatment of the LDH data in Figure 5 yields $\lambda = 0.58$, showing that LDH release includes a greater sensitivity to device surface interactions then does hemoglobin release; the corresponding coefficient is $\overline{K} = 5.18 \times 10^{-5}$ $mm^{-\lambda}\cdot min^{-1}$, with the sum of squared residuals also being 0.013.

The fact that hemoglobin and LDH release rates are characterized by different values of $\overline{K}$ and λ should not be surprising. One would expect them to be the same only if release occurred by cell rupture, which does not prevail under low-stress conditions. The parameter differences probably signify molecular size and cell binding differences. For example, the larger value of λ for LDH (0.58 vs. 0.36) may reflect the fact that LDH originates in the cell membrane (as well as in cytoplasm), while hemoglobin does not.

The influence of S/V in these tests is clearly not great. Indeed, from inspection of Figures 4 and 5 it is tempting to regard the data—as a first approximation—to be independent of S/V and merely a *power law* function of shear rate such as $\Delta c \propto \langle\dot{\gamma}\rangle^{\beta}$, in contrast to the linear form of Eq. 4b and the evidence of Figures 2 and 3. There is, after all, no physical argument that requires linearity in blood damage kinetics. Use of a least-squares procedure yields optimal values $\beta = 1.22$ (hemoglobin) and 1.52 (LDH), still not far from linear. However, poorer representations than Eq. 5 were obtained in each case, the sums of squared residuals being 0.026 and 0.016 for hemoglobin and LDH respectively. Thus, as a pragmatic matter, there is no incentive to dismiss S/V as a variable. Finally, with respect to the $\dot{\gamma}$-dependence, an overall best-fit procedure using $\Delta c \propto \langle\dot{\gamma}\rangle^{\beta}(S/V)^{\lambda}$ led to an optimal value $\beta = 1.04$. This is not significantly different from the linear case and encourages the latter to be retained hereafter.

It must be borne in mind that the parameters quoted above and Eq. 5 are only correlative, not mechanistic. Even at the simplest mechanistic level that can be envisioned, with two independent generators (surface and bulk) of damage operating in parallel, one needs a representation such as

$$\Delta c = \left[\left(\frac{S}{V}\right)\langle\dot{\gamma}\rangle_S \overline{K}_S + \langle\dot{\gamma}\rangle_B \overline{K}_B\right] \frac{t_o}{(1-H)} \tag{6}$$

In principle, $\overline{K}_S$ and $\overline{K}_B$ could be evaluated from the slope and intercept of plots of Δc vs. S/V. Sensitivity of Δc to S/V in Eq. 6 can range from linear to zero order (spanning the values of λ quoted above), depending on the relative magnitudes of the two contributions.

The data presented here, on 23-day-old blood, suggest that $\overline{K}_B > (S/V)\overline{K}_S$ in the context of Eq. 6, with $\overline{K}_B$ being about 2 to 8 times greater than $(S/V)\overline{K}_S$. This may well be the general case for older bloods, including those of legally transfusable age (less than 21 days old). Biomaterials effects would contribute through the sensitivity of $\overline{K}_S$ to device surface chemistry, and thus we can explain why materials influences are often less distinct in data on older bloods (Offeman and Williams, 1976). Note, however, that they would still play a major role when S/V is large. Fresher blood has lower Δc and hence lower $\overline{K}_S$ and $\overline{K}_B$, but the ratio $(S/V)\overline{K}_S/\overline{K}_B$ can be larger than for old blood and thus materials effects would be relatively more important.

Mechanisms of surface-induced shearing damage to blood are relatively easy to envision. Erythrocyte membranes may respond adversely to contact with the chemistries of synthetic surfaces, even if mediated with protein deposits. Sliding friction along a solid wall could create high membrane stress and deformation, allowing even large molecules to escape through locally enlarged pores. Momentary adhesion to the wall, followed by subsequent removal could be especially traumatic; Blackshear (1972) points out that the tether sometimes produced as the cell is withdrawn is a region of great membrane stretch and potential porosity. All these phenomena would be encompassed within $\overline{K}_S$ of Eq. 6.

It is more difficult to postulate mechanisms for independent bulk damage within the low-stress regime (which clearly pertains here, inasmuch as no abrupt threshold is seen in Figures 2–5, cell morphologies were not visibly altered, and stresses were truly low). Ordinary cell-cell friction should produce only small local membrane forces, and the relative freedom of cells to rotate in a shear field reduces the stress in their membranes far below what it would be if the cells were tethered to a wall. This means that even the sieving mechanism suggested for osmotic hemolysis (MacGregor, 1972), wherein membrane stretching allows pores to develop, is not probable here. It is possible, of course, that aged bloods contain a fraction of highly fragile erythrocytes that are severely damaged by these moderate cell-cell interactions. And, despite a low percentage of cells being damaged (and/or a small amount of damage per event), the total number of cell-cell events vastly exceeds the number of cell-wall events, so K_B could appear large compared to $K_S S/V$ in Eq. 6.

However, more subtle possibilities also exist as alternatives to the two parallel mechanisms of Eq. 6. A two-step series process, by which cells are first traumatized at the solid surface and then move out into the bulk fluid to discharge their components, could give a variety of results. Although the loss of hemoglobin, etc. would be occurring in the bulk, Δc would be dependent on (S/V) as long as surface-induced cell trauma were a continuing kinetic process while the flow was sustained. Alternatively, if the full extent of surface trauma occurred rather rapidly—and Blackshear (1972) has argued that tests of several minutes' duration at high shear rates should produce contact of virtually all cells with some portion of solid surfaces—then the (S/V) dependence would be lost at later times as hemolysis continued in bulk without further surface triggering. Over an intermediate time period, then, an appearance of $\Delta c \propto (S/V)^{\lambda}$ with $0 < \lambda < 1$ could arise from this behavior, as was found in the correlation of Eq. 5. The overall $\dot{\gamma}$-dependence would depend upon whether the activation step at the solid wall were purely chemical (independent of $\dot{\gamma}$) or influenced by surface shear (e.g., tether stretching), and also upon whether the subsequent component release were $\dot{\gamma}$-enhanced or proceeded at a rate dictated by its intrinsic recovery mechanisms (independent of $\dot{\gamma}$); any dependence from $\dot{\gamma}^0$ to $\dot{\gamma}^2$ could be seen in $\Delta c(\dot{\gamma})$ among these various cases. This series model suggests how the release of cell components in the bulk could be sensitive to the materials of device construction and their texture. Additional analysis of blood damage in terms of the series model for hemolysis will be presented elsewhere (Laugel and Beissinger, 1983).

Finally, it should be recalled that kinetic expressions such as Eqs. 3a and 4a are merely simple illustrations of how $\dot{\gamma}$-dependent effects can be incorporated at the lowest level. They do not distinguish between cell responses to shear deformation and tensile deformation; both are lumped together in the rate constants K_S and K_B. Further refinements in modeling will probably have to account for mechanistic differences in those cell responses.

In conclusion, we can say that some progress has been made in clarifying the dual role of solid surface effects and bulk fluid effects in shear-induced blood damage within the low-stress regime. The existence of hemolysis simultaneously on surfaces and in bulk had not previously been identified. However, the relative importance of these contributions cannot yet be predicted, and even the precise mechanisms involved must await further elucidation.

ACKNOWLEDGMENT

Financial support was provided by NIH grant No. 1-R01-HL23274 from the Devices and Technology Branch, Div. of Heart and Vascular Diseases of the National Heart, Lung, and Blood Institute. We are also grateful to Mary Meyers of the Blood Bank of Alameda-Contra Costa Counties, Oakland, for her help in providing blood samples. Henry Borsook of Santa Barbara was a source of constant inspiration and hematological expertise.

NOTATION

c = concentration in plasma, either mg/100 mL (for hemoglobin) or units/L (for LDH)
CP = cone and plate
H = hematocrit, erythrocyte volume fraction in blood sample
h = gap spacing between parallel plates, mm or cm
j = flux of hemoglobin (or LDH) moving from solid wall to plasma, mg/cm^2·s
K = rate coefficients for release of cell components due to shear, Eqs. 3a and 4a
$\overline{K}$ = time-average of K over period of shear (here, 10 min)
PP = parallel plate
R = radius of platen, cm
$\mathcal{R}$ = volumetric rate of release of cell components to plasma
r = radial coordinate, cm
S = surface area, cm^2
T = torque, g·cm^2/s^2
t = time of shearing, s or min
V = volume of sample in device
w = rate of component moving away from entire solid wall into plasma, mg/s
z = coordinate along axis of parallel plate device, cm

Greek Letters

$\dot{\gamma}$ = shear rate, absolute magnitude, s^{-1}
$\langle\dot{\gamma}\rangle$ = average shear rate, s^{-1}
$\dot{\gamma}_{ij}$ = component of shear rate tensor, s^{-1}
Δ = difference, as in $\Delta c \equiv c(t) - c_o$
ζ = $z(\Omega/\nu)^{1/2}$
λ = correlation parameter for S/V effects, Eq. 5
η = non-Newtonian viscosity in steady shear, Pa·s or cp
η^* = complex viscosity in small-amplitude sinusoidal shear = $\eta' - i\eta''$, Pa·s or cp
θ = polar angle in spherical geometry (CP), azimuthal angle in cylindrical geometry (PP)
ν = η/ρ, cm^2/s
π = 3.14159...
ρ = mass density, g/cm^3
τ = shear stress, absolute magnitude, Pa
τ_{ij} = component of stress tensor, Pa
ϕ = azimuthal coordinate in spherical geometry (CP)
ψ = $\pi - \theta_o$ = cone angle, rad
Ω = angular speed of platen rotation, rad/s
ω = radian frequency of shear oscillation, rad/s

Subscripts

B,S = bulk and surface quantities
HGB = hemoglobin
LDH = lactate dehydrogenase
ij = component of a tensor
o = baseline value, including all handling artifacts

Superscripts

o = limit of viscometric flow, with no secondary effects in the hydrodynamics

APPENDIX

Cone And Plate

Torque measurements, used for η determination, are relatively insensitive to the onset of secondary flows. Many studies have cast results in the form

$$T/T^o = 1 + f(\psi)\cdot Re^2 \qquad \text{(A1)}$$

where T^o is torque expected from the unperturbed primary flow corresponding to $\dot{\gamma}^o = \Omega/\psi$, and $Re = \rho\Omega R^2/\eta_o$. Cheng (1968) tabulated his empirical results in this fashion, and for the conditions of our study (i.e., $\psi = 0.00908$ rad, $\rho = 1.05$ g/cm^3, $\eta_o \approx 0.0335$ poise) we find he predicts a 2% excess torque at $\Omega = 40$ rad/s. Since our Ω_{max} was 37.7 rad/s, we understand that viscosity measurements were never significantly affected. The exact analysis by Turian (1972) suggests even a greater safety factor, since the use of our Ω_{max} in his version of Eq. A1 gives $T/T^o = 1.003$.

However, the intensity of shear is not entirely reflected by torque, inasmuch as radial flow components do not directly register in $T(Re,\psi)$. This is illustrated in Table A1 for the condition Ω_{max} and $r = R$, where we have used the work of Fewell and Hellums (1977) to compute and display all six nonzero components of $\dot{\gamma}_{ij}$ and the viscometric ideal $\dot{\gamma}^o_{\theta\phi}$. If the former are used to evaluate $\dot{\gamma} \equiv |\dot{\gamma}|$ as described in the text, the consequence is $\dot{\gamma}/\dot{\gamma}^o = 1.24$ when the components of both upper and lower surfaces are separately entered into the computation. More importantly, extreme values of $\dot{\gamma}_{\theta\phi}$ are found at the two surfaces, with $\dot{\gamma}_{\theta\phi}/\dot{\gamma}^o_{\theta\phi}$ having a maximum of 1.586 on the rotating surface and a minimum of 0.716 on the stationary one. Even if blood damage were linear with $\dot{\gamma}$, these results show that enhancement over the $\dot{\gamma}^o$ case would be found.

Fortunately, problems are minimal for the other discrete values of Ω selected here. For $\Omega = 18.85$ rad/s, $\dot{\gamma}/\dot{\gamma}^o < 1.05$ and for lower-Ω cases the primary flow is vastly dominant and ideal.

Parallel Plates

The hydrodynamics of rotating disks of infinite radius has been treated analytically by Lance and Rogers (1962), Mellor et al. (1968), and Homsy (1974). The latter work presented detailed numerical results that were used here. In the PP geometry, a separation of variables is possible so that $v_r = r\Omega F(\zeta)$, $v_\theta = r\Omega G(\zeta)$, $v_z = (\eta_o\Omega/\rho)^{1/2} H(\zeta)$ where $\zeta \equiv z(\rho\Omega/\eta_o)^{1/2}$. With the disk rotating at $z = h$, the components $\dot{\gamma}_{ij}(r,z)$ are obtained formally as shown in Table A2. Solution of the problem requires evaluation of the ζ dependence of the functions F, G, H; the reader is referred to the above-cited literature for perturbation expansions valid for small ζ and usable under conditions of these experiments.

A selection of numerical results is also given in Table A2, for the region of greatest secondary flows ($r = R$) and the highest rotational rate ($\Omega_{max} = 37.7$ rad/s); results shown correspond to the three values of h used here. It is striking that even under these most severe conditions only two independent components of $\dot{\gamma}_{ij}$ are ever sig-

TABLE A1. CONE AND PLATE SHEAR RATE COMPONENTS AT PLATEN RIM, FOR $\Omega_{max} = 37.7$ RAD/s*

Component	Shear Rates+, s^{-1}, at Surface $\theta = \pi$	$\theta = \pi - \psi$
$\dot{\gamma}^o_{\theta\phi} = \dot{\gamma}^o_{\phi\theta}$	4,154	4,154
$\dot{\gamma}_{\theta\phi} = \dot{\gamma}_{\phi\theta}$	2,803	7,311
$\dot{\gamma}_{\theta r} = \dot{\gamma}_{r\theta}$	#	623
$\dot{\gamma}_{r\phi} = \dot{\gamma}_{\phi r}$	#	478
$\dot{\gamma}_{\theta\theta} = \dot{\gamma}_{rr}$	#	249
$\dot{\gamma}_{\phi\phi}$	#	42

* $Re \equiv \rho\Omega R^2/\eta_o = 28{,}275$ using $\rho = 1.05$ g/cm^3, $\eta_o = 0.035$ g/cm·s, $R = 5$ cm; also $\psi = 0.00908$ rad.
+ Rotating surface at $\theta = \pi - \psi$. Stationary surface at $\theta = \pi$.
# Not available from work of Fewell and Hellums (1977), but believed to be very close to values in adjacent column.

TABLE A2. PARALLEL PLATE SHEAR RATE COMPONENTS* AT PLATEN RIM, FOR Ω_{max} = 37.7 rad/s

Component form (all r and z)	h = 0.25 mm			h = 0.50 mm			h = 1.00 mm		
	$z = 0$	$z = h/2$	$z = h$	$z = 0$	$z = h/2$	$z = h$	$z = 0$	$z = h/2$	$z = h$
$\dot{\gamma}^o_{z\theta} = \dot{\gamma}^o_{\theta z} = r\Omega/h$	7,540	7,540	7,540	3,770	3,770	3,770	1,885	1,885	1,885
$\dot{\gamma}_{z\theta} = \dot{\gamma}_{\theta z} = r(\Omega^3\rho/\eta_o)^{1/2}G'(z)$	7,537	7,532	7,554	3,734	3,734	3,906	1,580	1,574	2,937
$\dot{\gamma}_{zr} = \dot{\gamma}_{rz} = r(\Omega^3\rho/\eta_o)^{1/2}F'(z)$	−11	7	−16	−720	453	−1,077	−1,434	1,790	−2,154
$\dot{\gamma}_{r\theta} = \dot{\gamma}_{\theta r} = 0$	0	0	0	0	0	0	0	0	0
$\dot{\gamma}_{\theta\theta} = \dot{\gamma}_{rr} = 2\Omega F(z)$	0	~0	0	0	~0	0	0	−1	0
$\dot{\gamma}_{zz} = 2\Omega H'(z)$	0	~0	~0	0	~0	~0	0	2	~0

* Table entries in units of s^{-1}. Functions F, G, H are dimensionless. Material parameters are: ρ = 1.05 g/cm^3; η_0 = 0.035 g/cm-s; R = 5cm.

nificant—i.e., $\dot{\gamma}_{z\theta}$ and $\dot{\gamma}_{zr}$—although this was not the case for CP (Table A1). Moreover, if we compare the two geometries when they have comparable gap spacings (h = 0.50 mm for PP; h_R = 0.45 mm for CP in Table A1), we find that the primary $\dot{\gamma}_{ij}$ component varies far less across the gap in the PP case. However, the secondary $\dot{\gamma}_{ij}$ component is somewhat stronger for PP than for CP. Finally, the step to h = 1.00 mm in Table A2 shows considerable transverse variation in the primary gradient $\dot{\gamma}_{z\theta}$, reflecting the fact that a boundary layer flow has been established in the primary velocity v_θ. While this is comparably severe for the CP case in Table A1, the PP flow has a much stronger secondary component, with $\dot{\gamma}_{zr}$ nearly the same magnitude as $\dot{\gamma}_{z\theta}$.

Finally, it should be borne in mind that all hydrodynamic analyses used here fail to account for the presence of the air/liquid boundary at $r = R$ and the corresponding enhancement of shear in this region where fluid elements must change direction. This factor may lead to more severe $\dot{\gamma}$-induced blood damage in the region of the interface, even if the air/blood chemical contact plays no direct role.

LITERATURE CITED

Bacher, R. P., and M. C. Williams, "Hemolysis in Capillary Flow," *J. Lab. Clin. Med.*, **76**, 485 (1970).

Bernstein, E. F., "Certain Aspects of Blood Interfacial Phenomena—Red Blood Cells," *Fed. Proc.*, **30**, 1510 (1971).

Beissinger, R. L., and E. F. Leonard, "Sorption Kinetics of Binary Protein Solutions: General Approach to Multicomponent Systems," *J. Coll. Int. Sci.*, **85**, 521 (1982).

Beissinger, R. L., and M. C. Williams, "Effects of Blood Storage Age on Rheology and Low-Stress Hemolysis," *Biorheology*, in preparation.

Blackshear, P. L., "Mechanical Hemolysis in Flowing Blood," *Biomechanics: Its Foundations and Objectives*, Ch. 19, Eds., Y. C. Fung, N. Perrone, and M. Anliker, Prentice-Hall, Englewood Cliffs, NJ (1972).

Cheng, D. C., "The Effect of Secondary Flow on the Viscosity Measurement Using the Cone-and-Plate Viscometer," *Chem. Eng. Sci.*, **23**, 895 (1968).

Cox, W. P., and E. H. Merz, "Correlation of Dynamic and Steady Flow Viscosities," *J. Polym. Sci.*, **28**, 619 (1958).

Dintenfass, L., *Blood Microrheology*, Butterworths, London (1971).

Fewell, M. E., and J. D. Hellums, "The Secondary Flow of Newtonian Fluids in Cone-and-Plate Viscometers," *Trans. Soc. Rheol.*, **21**, 535 (1977).

Hellums, J. D., and C. H. Brown, "Blood Cell Damage by Mechanical Forces," *Cardiovascular Flow Dynamics and Measurements*, Ch. 20, Eds., N. H. C. Hwang and N. A. Norman, Univ. Park Press, Baltimore (1977).

Homsy, R. V., "Mass Transfer to a Plane Below a Rotating Disk," Ph.D. thesis, University of California, Berkeley (1974).

Lampert, R. H., and M. C. Williams, "Effect of Surface Materials on Shear-Induced Hemolysis," *J. Biomed. Mater. Res.*, **6**, 499 (1972).

Lance, G. N., and M. H. Rogers, "The Axially Symmetric Flow of a Viscous Fluid Between Two Infinite Rotating Disks," *Proc. Roy. Soc.*, **A266**, 109 (1962).

Laugel, J.-F., and R. L. Beissinger, "Low Stress Shear-Induced Hemolysis in Capillary Flow," *Trans Amer. Soc. Artif. Inter. Organs*, **29**, 158 (1983).

Leverett, L. B., J. D. Hellums, C. P. Alfrey, and E. C. Lynch, "Red Blood Cell Damage by Shear Stress," *Biophys. J.*, **12**, 257 (1972).

MacGregor, R. D., and C. A. Tobias, "Molecular Sieving of Red Cell Membranes during Gradual Osmotic Hemolysis," *J. Membr. Biol.*, **10**, 345 (1972).

Mellor, G. L., P. J. Chapple, and V. K. Stokes, "On the Flow Between a Rotating and a Stationary Disk," *J. Fluid Mech.*, **31**, 95 (1968).

Monroe, J. M., R. C. Lijana, and M. C. Williams, "Hemolytic Properties of Special Materials Exposed to a Shear Flow, and Plasma Changes with Shear," *Biomat., Med. Dev., Art Organs*, **8**, 103 (1980).

Monroe, J. M., D. E. True, and M. C. Williams, "Surface Roughness and Edge Geometries in Hemolysis with Rotating Disk Flow," *J. Biomed. Mater. Res.*, **15**, 923 (1981).

Nevaril, C. G., J. D. Hellums, E. C. Lynch, and C. P. Alfrey, "Physical Factors in Blood Trauma," *AIChE J.*, **15**, 707 (1969).

Nichols, A. R., "Shear-Induced Surface Hemolysis: Blood Protein Interactions," M.S. Thesis, University of California, Berkeley (1975).

Nichols, A. R., "Shear-Induced Surface Hemolysis: Blood Protein Interactions," M.S. thesis, University of California, Berkeley (1975).

Nichols, A. R., and M. C. Williams, "Suppression of Shear-Induced Hemolysis by Three Plasma Proteins," *Biomat., Med. Dev., Art. Organs*, **4**, 21 (1976).

Nyilas, E., E. L. Kupski, P. Burnett, and R. M. Haag, "Surface Microstructural Factors and Blood-Compatibility of a Silicone Rubber," *J. Biomed. Mater. Res.*, **4**, 369 (1970).

Offeman, R. D., and M. C. Williams, "Shear-Induced Hemolysis: Effects of Blood Chemistry (Including Aging in Storage) and Shearing Surfaces," *Biomat., Med. Dev., Art. Organs*, **4**, 49 (1976).

Offeman, R. D., and M. C. Williams, "Material Effects in Shear-Induced Hemolysis," *Biomat., Med. Dev., Art. Organs*, **7**, 359 (1979a).

Offeman, R. D., and M. C. Williams, "Observations on Shear-Induced Hemolysis," *Biomat., Med. Dev., Art Organs*, **7**, 393 (1979b).

Shapiro, S. I., and M. C. Williams, "Hemolysis in Simple Shear Flows," *AIChE J.*, **16**, 575 (1970).

Turian, R. M., "Perturbation Solution of the Steady Newtonian Flow in the Cone and Plate and Parallel Plate Systems," *IEC Fund.*, **11**, 361 (1972).

Walters, K., *Rheometry*, John Wiley & Sons, New York (1975).

Wielogorski, J. W., W. T. J. Davy, and R. J. Regan, "The Influence of Surface Rugosity on Hemolysis Occurring in Tubing," *Biomed. Eng.*, **11**, 91 (1976).

Manuscript received December 6, 1982; revision received June 28, and accepted July 1, 1983.